

Optimal Design for Noise Reduction in Interior Permanent Magnet Motor

Sang-Ho Lee¹, Jung-Pyo Hong¹, Woo-Taik Lee¹, Sang-Moon Hwang², Ji-Young Lee³, Young-Kyoun Kim⁴

¹Department of Electrical Engineering, Changwon National University, #9, Changwon, Gyeongnam, 641-773, Korea,

²Department of Mechanical Engineering, Pusan National University, Pusan, 609-735, Korea

³Transverse Flux Machine Research Group, Korea Electrotechnology Research Institute, Changwon, 641-120, Korea

⁴Power Electronics Group, Digital Appliance Business SAMSUNG ELECTRONICS CO.,LTD., 443-742, Korea

tapaya@korea.com, jphong@changwon.ac.kr, shwang@pusan.ac.kr

Abstract—This paper presents methods to reduce acoustic noise in interior permanent magnet (IPM) motor during design stage. Mechanical and magnetic sources are considered to reduce noise of the machine, and structural and electromagnetic designs are performed. In the structural design stage to reduce mechanical source, the structural resonances are moved to higher frequency for enhancement of stiffness. Then, the electromagnetic design stage to reduce magnetic source, the amplitudes of magnetic force harmonic and torque ripple are reduced by using an optimal design method, respectively. Two models are designed according to each objective function, and the validity of the design process and objective functions is confirmed with their simulated and experimental results.

Keywords—Acoustic noise, Equivalent magnetizing current, Harmonic, IPM, Magnetic force, Objective function, Optimal design, Stiffness

I. INTRODUCTION

Noise sources in electric machines are broadly categorized as magnetic, mechanical, electronic, and aerodynamic sources [1]. Generally, the mechanical and magnetic sources are considered as main noise sources of electric motors [2-4] because the interaction between the harmonic of magnetic forces and the resonant frequency of mechanical structure is the major cause of vibration which produces the noise. Although torque pulsations and tangential components of magnetic force also contribute to vibration and magnetic noise, normal components are larger than the tangential one in general [5].

Concentrated winding type of interior permanent magnet (IPM) motors have more advantages such as short end turns, low copper loss, and effective high-volume automated manufacturing than distributed winding type [2]. However, back electromotive force (BEMF) and current have many harmonic components, because flux in concentrated winding type concentrates on stator pole. In addition, torque ripple is relatively large compared with distributed winding type.

In this paper, the design process consists of the structural and electromagnetic designs to reduce acoustic noise of prototype which is BLDC IPM motor with concentrated winding. In the structural design stage to reduce mechanical source, structural resonances are moved to higher frequency to enhance the stiffness of the stator. The quantity of vibration

according to design variables of the stator is expressed by sound pressure level (SPL) which is calculated by using boundary element method (BEM). To reduce the SPL, a new stator structure enhancing the stiffness is decided. Then, electromagnetic design stage, to reduce magnetic sources, the amplitudes both harmonic of magnetic forces affects stator pole and torque ripple are reduced by using an optimal design method, respectively. In the optimal design using response surface methodology (RSM), two effective objective functions are proposed [6]. Therefore, two models are designed according to each objective function, and the simulated and experimental results of the models are compared with the prototype. The validity of the design process and objective functions is confirmed with the results.

II. THEORY

A. Mechanical system and resonant frequency

The mechanical system can be simply described with N degrees of freedom in the following matrix form

$$[M]\{\ddot{q}\} + [C]\{\dot{q}\} + [K]\{q\} = \{F(t)\} \quad (1)$$

where q is an $(N,1)$ vector expressing the displacement of N degree of freedom, $[F(t)]$ is the force vector applying to the degrees of freedom, $[M]$ is the mass matrix, $[C]$ is the damping matrix, and $[K]$ is the stiffness matrix.

Calculation of resonant frequencies of the stator is essential in the vibration analysis of electric machine. The resonant frequency of the stator system of the m th circumferential vibration mode can be expressed as:

$$f_m = \frac{1}{2\pi} \sqrt{\frac{K_m}{M_m}} \quad (2)$$

where K_m is the lumped stiffness (N/m) and M_m is the lumped mass (kg) of the stator system.

As the result of the vibration, the surface of the stator yoke displaces with frequencies corresponding to the frequencies of magnetic forces [5].

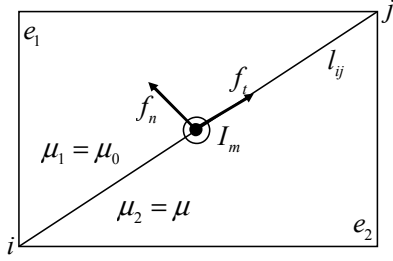


Fig. 1. Magnetizing current between two materials.

B. Magnetic force calculation

Fig. 1 shows the magnetizing current between two materials. As one of the method of magnetic force calculation, equivalent magnetizing current (EMC) method uses magnetizing current which exists on element boundary and it can directly calculate the electromagnetic force which affects the surface of structure. The current I_m on the line forming element e_1 and e_2 is written as eq. (3)

$$I_m = \frac{1}{\mu_0} \int \nabla \times \bar{M} \cdot d\bar{s} = \frac{1}{\mu_0} (M_{1t} - M_{2t}) l_{ij} \quad (3)$$

where M_{1t} and M_{2t} are the tangential components of magnetization on element boundary, l_{ij} is the distance on element boundary.

$$\bar{B} = \mu_0 \bar{H} + \bar{M} \quad (4)$$

The relationship in eq. (4) holds for all materials whether they are linear or not [7]. Substituting eq. (4) into eq. (3) yields

$$I_m = \frac{1}{\mu_0} (B_{1t} - B_{2t}) l_{ij} \quad (5)$$

where B_{1t} and B_{2t} are the tangential component of flux density in each material.

The electromagnetic force on the element boundary is written as

$$\bar{f}_{ij} = I_{ij} \times \bar{B}_{ext} \quad (6)$$

Flux density value of \bar{B}_{ext} is given as the average value for each element.

III. CHARACTERISTICS OF PROTOTYPE

The specifications and resonant frequencies of stator in prototype model are listed in Table I. The resonant frequency of stator is changed depending on assembly because of the different stiffness.

Fig. 2 shows a configuration of noise experiment in the anechoic room where background noise is 41dBA and measured 1m away from the motor by microphone. As a load of IPM motor, generator coupled with IPM motor produces the active power at the resistance.

The measured noise spectra of the prototype according to driving frequency are shown in Fig. 3. There are three major frequency bands, S1, S2, and S3. The frequency band S1 is

moving proportional to driving frequency, and it is considered as an effect of commutation, that is phase current switching. On the other hand, the frequency band S2 is fixed, and it is considered as an effect of structural resonance. The frequency band S3 is spreading, and it is considered as an effect of PWM frequency.

The factors of these three effects correspond to magnetic, mechanical, and electronic sources, respectively. Therefore, the frequency bands S1 and S2 are considered in order to reduce the noise induced by magnetic and mechanical sources. At the rated speed of 3000rpm, mechanical frequency is 50Hz, the frequency band S1 is partially overlapped to S2, and all resonant frequencies of stator in Table I are included in the band between S1 and S2. In consideration of this result, the frequency band 1.8~2.6kHz is regarded as main frequency band to reduce acoustic noise at the rated speed.

TABLE I. SPECIFICATIONS AND RESONANT FREQUENCIES OF STATOR.

| Contents | | Values |
|--------------------------------------|--------------------------------------|--------|
| Number of poles slots | | 4/6 |
| Rated current (A_{rms}) | | 13.0 |
| Series turn number per phase (turns) | | 65 |
| Rated speed (rpm) | | 3000 |
| Rated torque (kgf-cm) | | 80.0 |
| PWM frequency (kHz) | | 4.0 |
| Resonant frequency of stator (kHz) | Stator only | 1.5 |
| | Assembly of stator and housing | 1.8 |
| | Assembly of stator, housing, and Jig | 2.6 |

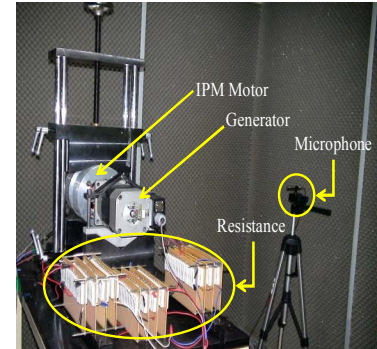


Fig. 2. Configuration of noise experiment.

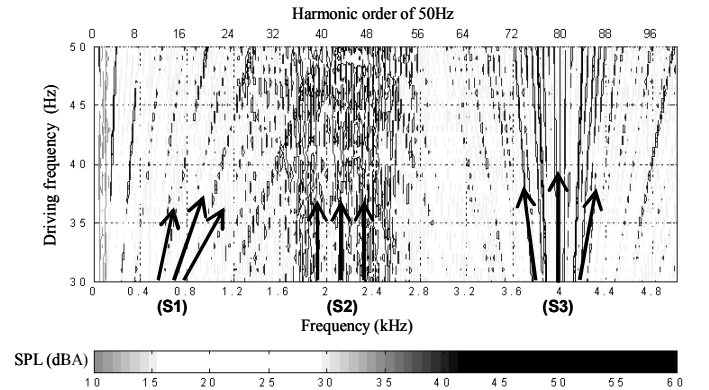


Fig. 3. Noise spectra according to driving frequency and three major frequency band under rated torque.

IV. DESIGN PROCESS

The design process consists of structural and electromagnetic designs. First, the structural design is performed to enhance the stiffness of the stator. Then, electromagnetic design is followed by using an optimal design to reduce the harmonic of magnetic forces and torque ripple.

A. Structural design

In the structural design stage, there are three basic assumptions as follows.

- i) The kinetic energy of the air layer on the stator surface is the vibration energy of the stator, and it is calculated by vibration analysis using finite element method.
- ii) The velocity of the stator vibration is the source of noise.
- iii) The object of structural design is reducing SPL calculated by noise analysis using BEM, and the reduction of SPL is interpreted as the enhanced stiffness.

Fig. 4 shows the design variables, which are tooth width (TW), tooth angle (TA), tooth height (TH), link thickness (LT), and yoke thickness (YT). According to change for each design variables, resonant frequencies of stator using modal analysis compared with prototype are expressed in Table II. LT and YT are main effective design variables to increase the resonant frequency.

When the exciting force on the center of tooth surface is equal to 1N, Fig. 5 shows the resonant frequency, vibration, and noise analysis results of prototype, M_LT, and M_YT which are changed by increment of LT and YT, respectively. These results note two important facts as follows.

- i) Both vibration and noise can be decreased when resonant frequency is increased by design variables.
- ii) If each mass is different and their kinetic energies are the same, the noise value can be different although the vibration is the same such as the example M_LT and M_YT in Fig. 5.

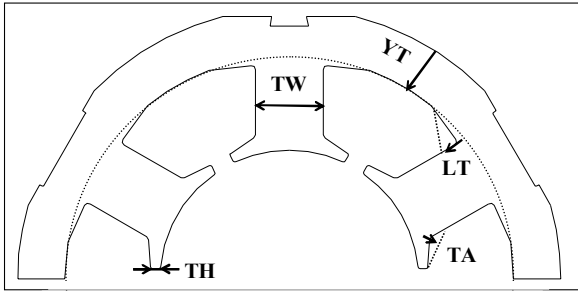


Fig. 4. Design variables in structural design.

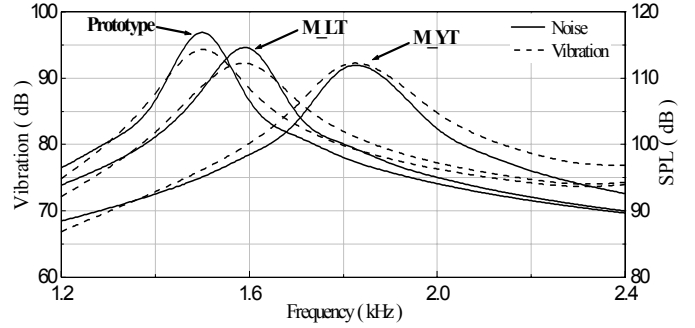


Fig. 5. The comparison of resonant frequency, vibration, and noise spectrum.

As the results of noise analysis for each design variable, LT and YT are the major influences on SPL variation. Therefore, LT and YT are used to find the optimal point, which is the increase in the resonant frequency of first circumferential vibrational mode to enhance the stiffness. As the constraint condition, the values of fill factor are between 35% and 40% to get the same turn number per phase of prototype. In addition, the external diameter of stator is constant.

The predicted response surface using modal analysis is drawn as shown in Fig. 6, the optimal point considering constraint condition is found at the point in which LT and YT are 3.3 and 4.2mm, respectively. The values of predicted first circumferential vibrational mode by RSM and calculated by FEM are 1.83 and 1.88 kHz, respectively.

Fig. 7 shows the result of structural design using RSM. As the optimized stator shape for enhancement of the stiffness, the black area means the expansion of core compared with prototype. Accordingly, structural design to reduce the acoustic noise in electric machines focuses on the enhancement of the structural stability and stiffness using LT and YT.

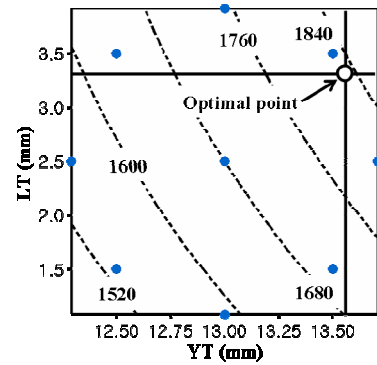


Fig. 6. Design variables in structural design.

TABLE II. RESONANT FREQUENCY OF STATOR ACCORDING TO DIMENSION VARIATION.

| Model name | Prototype | M_TH | M_TA | M_TW | M_YT | M_LT |
|---------------------|-----------------------------------|----------------|-----------------|-----------------|------------------|----------------|
| Dimension variation | - | 2.5 → 1.5 (mm) | 15.0 → 25.0 (°) | 17.5 → 19.5(mm) | 12.1 → 14.1 (mm) | 1.5 → 3.0 (mm) |
| Mode number | 1 st , 2 nd | 1503 | 1523 | 1492 | 1503 | 1843 |
| | 3 rd | 3370 | 3454 | 3325 | 3339 | 4265 |
| | 4 th | 4339 | 4387 | 4311 | 4436 | 5257 |

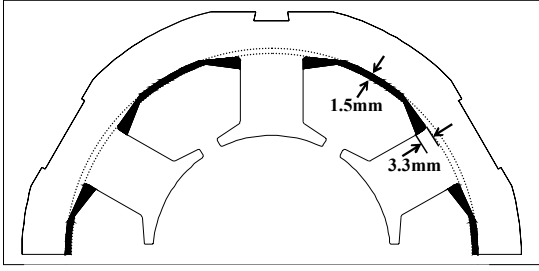


Fig. 7. Optimized stator shape by structural design.

B. Electromagnetic design

After structural design, the prototype with the optimized stator shape is the initial model for electromagnetic design.

Fig. 8 shows the electromagnetic design process using Design of Experiment (DOE) and RSM as an optimal design method. In the first stage using DOE, several design variables and areas are examined whether they have influence on magnetic forces. And then, the optimal design is performed with main effective design variables and two effective objective functions. The proposed two objective functions and the constraint condition are defined as follows:

Objective function:

$$F_{obj1} = K_{normal} + K_{tangential} \quad (7)$$

$$F_{obj2} = Torque\ ripple \quad (8)$$

$$K = 10 \log \sum_{i=1}^{10} \frac{(F_R + F_A + F_W)}{10} \quad (9)$$

Subject to:

$$T_{avg} \geq 80.0\ kgf - cm \quad (10)$$

where K_{normal} is K for the harmonic of normal force, $K_{tangential}$ is K for the harmonic of tangential force, F_R is the harmonic of magnetic forces, F_A is the A-weighting in weighting frequency curves [8], F_W is the weighting factor for 1.8~2.6 kHz which is the main resonant frequency band, and T_{avg} is the average torque.

These two objective functions are made to investigate which component between the harmonic of magnetic forces and torque ripple mainly affects noise.

The design variables, which are bridge width(BW), chamfer(CF), pole angle(PA), slot open(SO), and tooth height (TH) in Fig. 9 are selected. CF shape is shown in Fig. 10. Design variables are designated by x and y , because CF shape has several kinds of the combination. The interval of x is 0.5mm from the tooth end adjacent air-gap and full factorial design is performed with BW.

Except for CF, fractional factorial design is applied to obtain significantly design variables for two objective functions in screen activity stage and BW, PA and SO are selected as the main and interaction effects [9]. To simplify and avoid complexity of RSM, response surface using central composite design (CCD) is firstly performed by PA and SO which have

the highest effect. And then, optimal design based on the response surface results is performed by BW and CF.

Table III shows the design areas of PA and SO for response and Fig. 11 shows the response surface results, which have different aspects between the harmonic of magnetic forces and torque ripple. A point only reduces the harmonic of magnetic forces under the similar torque ripple of prototype and B point is a compromise between the harmonic of magnetic forces and torque ripple compared with prototype.

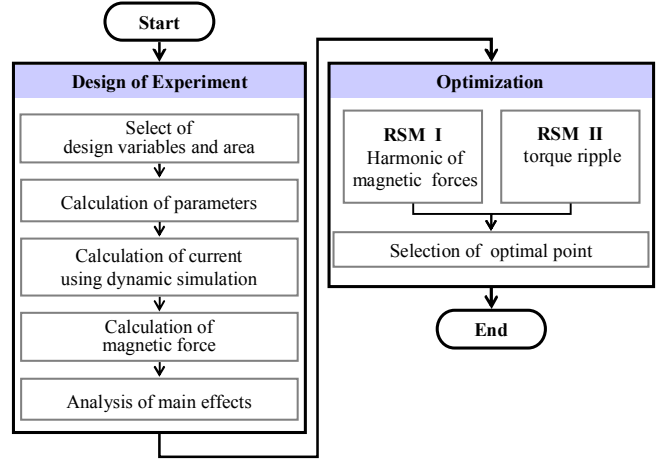


Fig. 8. Electromagnetic design process.

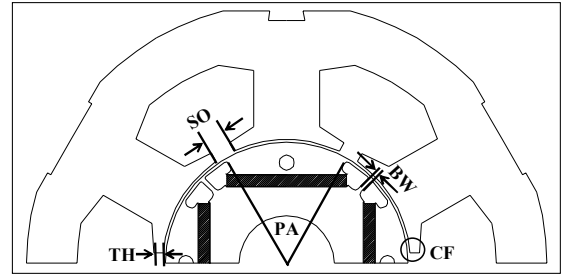


Fig. 9. Design variables in electromagnetic design.

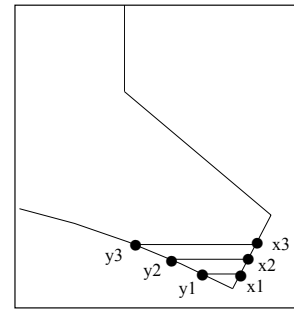


Fig. 10. Chamfer(CF) shape.

TABLE III. DESIGN VARIABLES AND AREAS FOR RESPONSE TWO OBJECTIVE FUNCTIONS.

| Design variables | unit | Coded values | | | | |
|------------------|------|--------------|------|------|------|-------|
| | | -1.682 | -1.0 | 0 | 1.0 | 1.682 |
| Pole angle (PA) | ° | 50.08 | 53.4 | 61.4 | 69.4 | 72.71 |
| Slot open (SO) | mm | 3.89 | 4.35 | 5.45 | 6.55 | 7.00 |

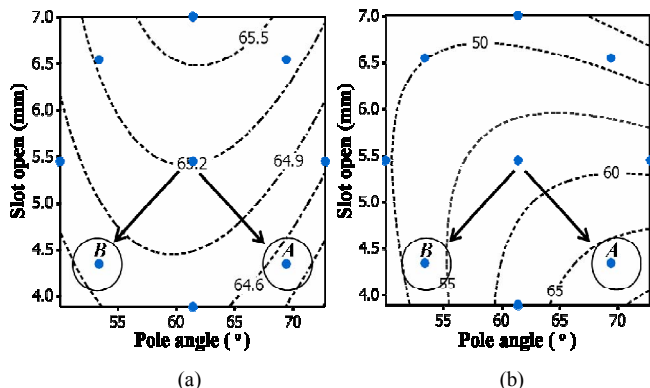


Fig. 11. Response surface (a) Harmonic of magnetic forces, (b) Torque ripple.

As the model of *A* point, the initial FR model is designed on the assumption that the harmonic components of magnetic forces have influence, and optimized for the first objective function F_{obj1} to be reduced. On the other hand, the initial TFR model which is the *B* point is designed on the assumption that the component of torque ripple has influence, and optimized for the second objective function F_{obj2} to be reduced.

After the initial design using PA and SO, the optimal design results for FR and TFR using BW and CF are shown in Fig. 12. BW and CF of two optimized models are the same shape, which is 2.5mm and the combination of x_2 and y_3 in Fig. 10, respectively.

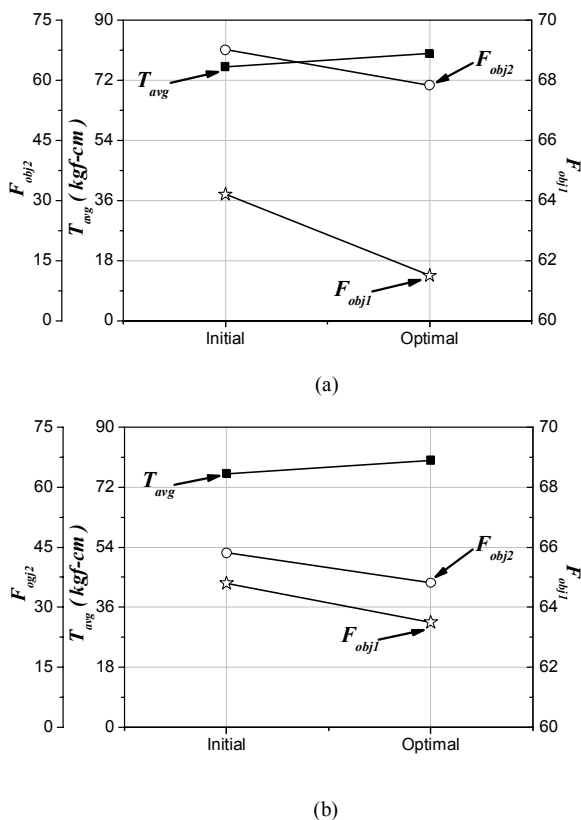


Fig. 12. The results of optimal design (a) FR, (b) TFR.

TABLE IV. THE COMPARISON OF SHAPE ACCORDING TO MODEL.

| Model name | Design variables | | |
|------------|------------------|--------|---------|
| | BW (mm) | PA (°) | SO (mm) |
| Prototype | 0.5 | 55 | 5.5 |
| FR | 2.5 | 72 | 4.3 |
| TFR | | 53 | |

The dimension of design variables according to model is shown in Table IV. Two optimized models have the same BW and SO. As the main and interaction effect, PA and SO of electric machines having high power density such as IPM motors lead to the different characteristic for the harmonic of magnetic forces and torque ripple.

V. ANALYSIS AND EXPERIMENTAL RESULTS

Fig. 13 shows the comparison of design results for prototype, FR, and TFR. FR has the lowest harmonic of magnetic forces among the models but torque ripple is similar to prototype. F_{obj1} of FR is almost 8.0% lower than prototype. TFR compared with prototype has low torque ripple and the harmonic of magnetic forces. F_{obj1} and F_{obj2} of TFR compared with prototype are reduced about 32.0 and 4.5%, respectively.

Fig. 14 shows the noise experiment results measured by 1/3 octave band at the 3000rpm and 80kgf-cm. Total SPLs of the two designed models compared with prototype are entirely reduced and the values of prototype, FR, and TFR are 76.5, 71.4, and 73.2dBA, respectively. The noise of two optimized models mainly occurs around the resonant frequency of stator and the noise of TFR around 4.0kHz is higher than FR. The reason is that inductance of TFR is lower than FR due to magnetic saturation according to reduction of pole angle. Therefore, current waveform of TFR more exactly reflects PWM characteristic and the noise at PWM frequency band is more highly measured than FR.

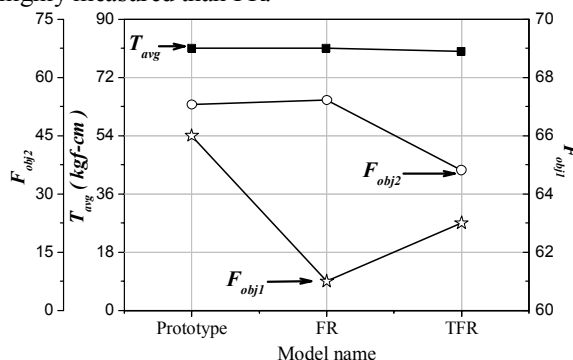


Fig. 13. The characteristic between prototype and two optimized models.

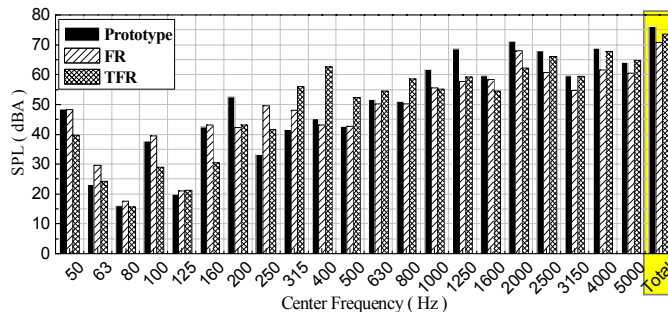


Fig. 14. Noise experiment result (@ 3000rpm, 80kgf-cm).

VI. DISCUSSION

In order to reduce the acoustic noise in IPM motor, structural and electromagnetic design process are introduced in this paper. Especially, two effective objective functions which are divided into the harmonic of magnetic forces and torque ripple are proposed in electromagnetic design.

Two models are designed according to each objective function, and the simulated and experimental results are compared with the prototype. From the noise experiment, the noise of optimal model designed by objective function using the harmonic of magnetic forces is more reduced than another. Accordingly, objective function using the harmonic of magnetic forces is more effective to reduce the noise.

In conclusion, the structural design should focus on vibration reduction by increasing stiffness and stability of stator. And then the electromagnetic design should pay more attention to harmonic reduction of magnetic forces which affects stator pole.

ACKNOWLEDGMENT

This work was supported by grant No. RTIO04-01-03 from the Regional Technology Innovation Program of the Ministry of Commerce, Industry and Energy(MOCIE).

REFERENCES

- [1] M. N. Anwar and Iqbal Husai, "Radial Force Calculation and Acoustic Noise Prediction in Switched Reluctance Machines." *IEEE Trans., on Ind. Applicat.*, Vol. 36, No. 6, pp. 1589-1597, Nov./Dec. 2000
- [2] C. C. Hwang, S. P. Cheng, C. M. Chang, "Design of High-Performance Spindle Motors with Concentrated winding," *IEEE Trans., Magn.*, Vol.41, No.2, pp.971-973, Fbr, 2005.
- [3] Jung-Pyo Hong, Kyung-Ho Ha, and Ju Lee, "Stator pole and yoke design for vibration reduction of switched reluctance motor," *IEEE Trans., Magn.*, Vol. 38, No. 2, pp.929-932, Mar. 2002.
- [4] G. Henneberger, P. K. Sattler, D. shen, "Nature of the equivalent magnetizing current for the force calculation," *IEEE Trans., Magn.*, Vol. 28, No. 2, pp.1068-1072, Mar. 1992.
- [5] Jacek F. Gieras, Chong Wang, Joseph Cho Lai, *Noise of Polyphase Electric Motors*, CRC press, 2006.
- [6] Kyung-Ho Ha, Youn-Kyoun Kim, Geun-Ho Lee, and Jung-Pyo Hong, "Vibration Reduction of Switched Reluctance Motor by Experimental Transfer Function and Response Surface Methodology," *IEEE Trans., Magn.*, Vol. 40, No. 2, pp.577-580, Mar. 2004.
- [7] Matthew N. O. Sadiku, *Elements of Electromagnetics*, Oxford Univ. press, 2001.
- [8] Nau, S.L., Mello, H.G.G., "Acoustic noise in induction motors: causes and solutions," Petroleum and Chemical Industry Conference, 2000. Industry Applications Society 47th Annual Conference Paper, pp.253-263, 11-13, Sept, 2000
- [9] Sung-II Kim, Jung-Pyo Hong, Young-Kyoun Kim, Hyuk Nam, Han-Ik Cho, "Optimal design of Slotless-Type PMLSM considering Multiple Response by Response Surface Methodology," *IEEE Trans. Magn.* Vol. 42, No. 4, pp.1219-1222, April, 2006.